BBA - Bioenergetics 1860 (2019) 148059

Contents lists available at ScienceDirect

BBA - Bioenergetics

journal homepage: www.elsevier.com/locate/bbabio

Mechanism of protonation of the over-reduced Mn_4CaO_5 cluster in photosystem II

Keisuke Saito, Hiroshi Ishikita*

Research Center for Advanced Science and Technology (RCAST), The University of Tokyo, 4-6-1 Komaba, Meguro-ku, Tokyo 153-8904, Japan
Graduate School of Engineering, The University of Tokyo, 4-6-1 Komaba, Meguro-ku, Tokyo 153-8904, Japan

ARTICLE INFO

Keywords:
Radiation damage
X-ray dose
Proton transfer
Low-barrier hydrogen bond
Jahn-teller effect

ABSTRACT

Based on characterization by X-ray absorption spectroscopy, it has been proposed that the Mn_4CaO_5 cluster in the crystal structure of the water-oxidizing enzyme, photosystem II (PSII), may represent an over-reduced form arising from reduction by the X-ray beam. Using a quantum mechanical/molecular mechanical approach, and assuming that all of the μ-oxo bridges are deprotonated in S_1, we analyzed the reduction process of the Mn_4CaO_5 cluster. In the crystal structure, the O atom (O5), which is linked with three Mn atoms and one Ca atom, has no H-bond. When reduced to S_{-2}, unexpectedly, a water molecule at Ca^{2+} (W3) reoriented itself, formed a H-bond with O5, and released a proton to O5, resulting in formation of OH^- at both W3 and O5. Once generated, the OH^- group at O5 was stable, because the W3…O5 H-bond had already disappeared. A weak binding of H_2O at Ca^{2+} led W3 to reorient and serve as a proton donor to O5 upon over-reduction.

1. Introduction

In photosystem II (PSII), the Mn_4CaO_5 cluster catalyzes the water splitting reaction: $2H_2O \rightarrow O_2 + 4H^+ + 4e^-$. The release of protons has been observed in response to changes in the oxidation state (the S_n state, where the subscript represents the number of oxidation steps accumulated) of the oxygen-evolving complex with a typical ratio of 1:0:1:2 for the $S_0 \rightarrow S_1 \rightarrow S_2 \rightarrow S_3 \rightarrow S_0$ transitions, respectively [1–3]. The PSII crystal structure reported at a resolution of 1.9 Å shows that water molecules W1 and W2 are ligands to the Mn4 atom of the Mn_4CaO_5 cluster, and W3 and W4 are ligands to the Ca atom [4,5] (Fig. 1). Based on the geometry, Umena et al. have proposed that W3 may be OH^- [4]. In the Sr-substituted PSII crystal structure, the W3–—Sr bond in the Mn_4SrO_5 cluster was specifically longer than the W3–—Mn bond in the unsubstituted Mn_4CaO_5 cluster [6]. Thus, Koua et al. have proposed that W3, rather than W4, may be a substrate water molecule [6].

Yano et al. [7,8] and Dau et al. [1,9] have argued that the atomic coordinates of the 1.9-Å structure [4] are in conflict with the X-ray absorption spectroscopy (XAS) data collected at a lower X-ray dose, and suggested that the PSII crystal structure may have been over-reduced (e.g., up to S_{-3}) during crystallographic data collection, resulting in the elongation of Mn–—O bonds. Theoretical studies have also suggested that the PSII crystal structure may be a mixture of over-reduced states, e.g., S_{-1} and S_{-2} [10–15]. Although over-reduced forms seem likely to be more protonated to compensate for the excess negative charge (see discussion in [16]) and a number of possible protonation patterns in the over-reduced forms have been investigated in theoretical studies in the absence of the PSII protein environment (e.g., by Galstyan et al. [14] and Krewald et al. [17], Fig. 2), little is known about the source of the proton and the mechanism of Mn_4CaO_5 protonation by the PSII protein environment. For example, i) Krewald et al. analyzed the over-reduced states, using a simplified computational model, which lacks not only D1-Val185 but also, e.g., D1-Asn298, D2-Lys317, and Cl^-. Accordingly, the absence of even the electrostatic interactions between the Mn_4CaO_5 cluster and these key components indicates that the simplified model do not correspond to native PSII but the D1-Val185-lacking [18], D1-Asn298-lacking [19,20], D2-Lys317-lacking [21], and Cl^--depleted [22] PSII (Fig. 2). ii) The simplified model used by Krewald et al. [17] is essentially identical to that used by Pantazis et al. [23] and Lohmiller et al. [24]. These simplified models assume that W2 is OH^- even in the absence of the strong proton acceptor in the PSII protein environment. However, it has been shown that W2 is most likely H_2O in S_1 and S_2, using polarized attenuated total reflectance Fourier transform infrared (ATR-FTIR) spectroscopy [25]. W2 = H_2O is consistent with the models proposed in Refs. [10,26]. iii) In the simplified model [23], the open-cubane and closed-cubane S_2 conformations were isoenergetic, whereas in most theoretical studies, the open-cubane S_2 conformation [i.e.,

* Corresponding author at: Research Center for Advanced Science and Technology (RCAST), The University of Tokyo, 4-6-1 Komaba, Meguro-ku, Tokyo 153-8904, Japan.
E-mail address: hiro@appchem.t.u-tokyo.ac.jp (H. Ishikita).

https://doi.org/10.1016/j.bbabio.2019.148059
Received 29 March 2019; Received in revised form 18 July 2019; Accepted 2 August 2019
Available online 05 August 2019

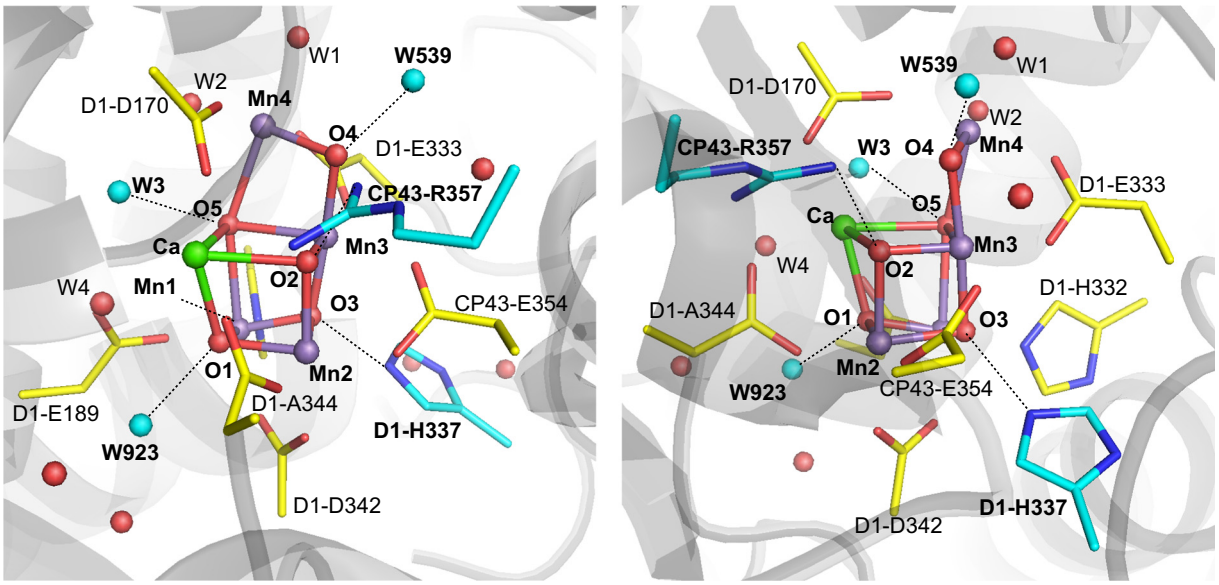

Fig. 1. Overview of the Mn_4CaO_5 cluster in the 1.9-Å crystal structure [4]. H-bond donor groups investigated are in cyan. Other water molecules (red) and Mn_4CaO_5 (purple, green, and red for Mn, Ca, and O atoms, respectively) are depicted as balls or sticks. H-bonds or ionic interactions are represented by dotted lines.

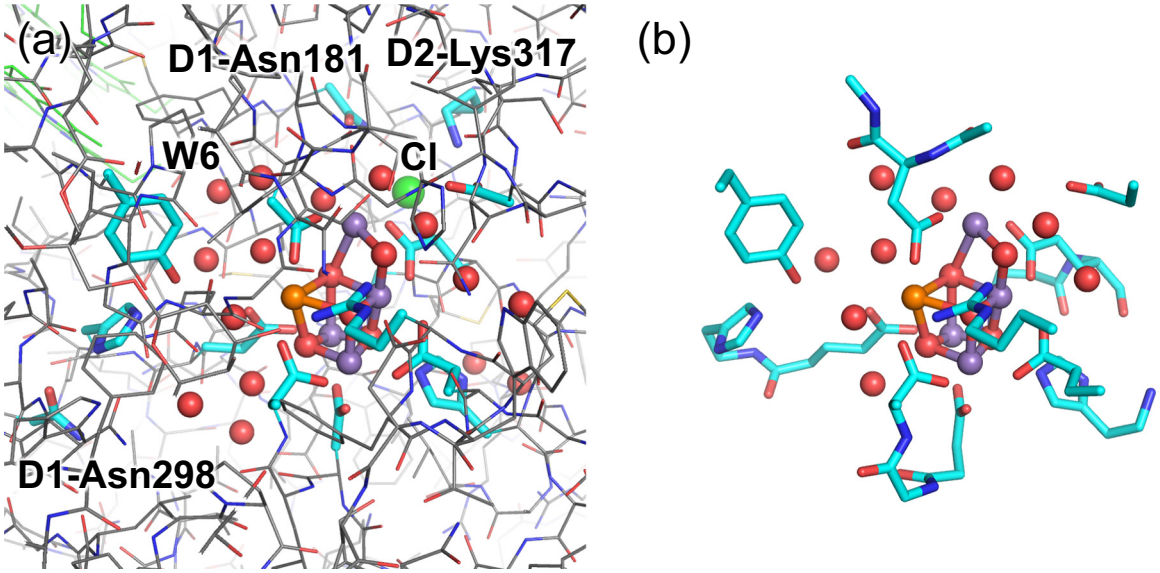

Fig. 2. (a) Computational model used in the present work, which has the PSII protein environment. The QM region is depicted as balls or sticks, whereas the MM region is depicted as lines. (b) Computational model used by Krewald et al. [17], which has no PSII protein environment. This model lacks not only D1-Val185 but also, e.g., D1-Asn298, D2-Lys317, and Cl^-.

(Mn1, Mn2, Mn3, Mn4) = (III, IV, IV, IV)] is energetically more stable than the closed-cubane S_2 conformation [i.e., (Mn1, Mn2, Mn3, Mn4) = (IV, IV, IV, III)] [27–30]. The discrepancy indicates that the simplified model does not sufficiently represent the PSII protein environment and does not reproduce the redox potential values for Mn1 and Mn4.

The protonation sites of the Mn_4CaO_5 cluster are five O atoms, O1 to O5 (Fig. 1). O1 to O4 each have corresponding H-bond donors: a water molecule (W923) for O1, CP43-Arg357 for O2, D1-His337 for O3, and a water molecule (W539) for O4. Only O5 has no H-bond partner in the original PSII crystal structures [4,31], which possibly indicates that O5 can be excluded from the candidates of plausible protonation sites. Although it has been reported that both W2 and W3 are within "the H-bond distances to O5" (i.e., O…O < ~3 Å) [4], this does not necessarily suggest that O5 forms a H-bond with W2 or W3. Indeed, the H…O…H angles between W2/W3 and O5 do not allow them to form a proper H-bond in physiological S states (e.g., S_0 and S_1) [32,33]. The absence of a proper H-bond makes proton transfer from O5 unlikely in the physiological S states, as suggested by theoretical studies [33,34] and time-resolved infrared measurements [35]. It should be noted that to propose the O5 deprotonation mechanism in the S_0 to S_1 transition, Siegbahn removed the hydrophobic D1-Val185 side-chain near O5 and twisted the ligand D1-His332 side-chain near O5 by 90° to create a space near O5 and add an extra water molecule [36]. As far as we are aware, there is no report that could directly demonstrate the release of the proton from O5 in the S_0 to S_1 transition in the presence of the PSII protein environment, without significantly manipulating the original geometry of the PSII crystal structures. Theoretical studies by Pal et al. [32] show that deprotonation of OH^- at O5 was not observed in the S_0 to S_1 transition because of the absence of the H-bond partner of O5 in the PSII protein environment (i.e., "the QM/MM S_0 model [32]"). Only when they used "a small model of the oxidized S_0' state [32]" with

W2 = OH^-, deprotonation of OH^- at O5 was possible. However, as already mentioned, ATR-FTIR studies suggested that W2 is not OH^- but H_2O [25]. It seems likely that deprotonation of O5 in the S_0 to S_1 transition is possible only in the absence of the PSII protein environment (e.g., [17,24,36]).

On the other hand, O4 forms a H-bond with a chain of water molecules, the O4-water chain. Theoretical studies have suggested that the O4-water chain facilitates the release of a proton from a μ-oxo of O4 in the S_0 to S_1 transition [33,34]. Recent time-resolved infrared measurements by Shimizu et al. showed that the S_0 to S_1 transition is the fastest (45 μs) among S-state transitions with a small value of 1.2 for kinetic isotope effect [35].They concluded that deprotonation of O4, which has the O4-water chain as a proton transfer pathway [33,34], is more consistent with their results than deprotonation of O5 [32,36]. Recently, Zhang et al. [37] and Chen et al. [38] reported the artificial Mn_4CaO_4 clusters with exchangeable solvent molecules. Because in all of the artificial Mn_4CaO_4 clusters, O5 was present but O4 was absent, they concluded that O5 in the cubane region is a structurally important component in the artificial Mn_4CaO_4 clusters and O4 could be a possible substrate site [38]. W1 can form a low-barrier H-bond with D1-Asp61 in higher S states [39], and the proton released from W1 via D1-Asp61 is likely to be released along the D1-Glu65/D2-Glu312 channel [40].

Although O4 [33,34] and W1 [39] are involved in long proton-transfer pathways that connects the Mn_4CaO_5 cluster with the protein bulk surface, these *physiological* proton transfer pathways may not necessarily be used for protonation of an over-reduced Mn_4CaO_5 cluster during crystallographic data collection. Galstyan et al. [14] demonstrated that upon over-reduction, O3 can be protonated by the release of a proton from the H-bond partner D1-His337 [14], without using physiological proton transfer pathways. As the pK_a value of a titratable residue is lowered when the residue is closer to the Mn_4CaO_5 moiety [41], proton transfer from the protein bulk surface to the reduced Mn_4CaO_5 cluster via the long physiological proton transfer pathways is less advantageous. In addition, the driving force for the formation of a low-barrier H-bond is provided by changes in the Mn_4CaO_5 reduction state (not changes in the bulk state) [34]. Therefore, a proton is more likely to be provided by the direct H-bond partner of the Mn_4CaO_5 cluster, in particular upon over-reduction. For proton transfer, formation of a low-barrier H-bond [42–44] with an over-reduced Mn_4CaO_5 cluster is prerequisite. Formation of a low-barrier H-bond cannot be judged only by the H-bond distances, but should be evaluated by the potential-energy profile, as pointed out by Schutz and Warshel [43]. As far as we are aware, the potential-energy profiles of the H-bonds of the over-reduced Mn_4CaO_5 cluster have not been reported in the presence of the PSII protein environment.

Here, we analyzed the reduction processes of the deprotonated S_1-Mn_4CaO_5 cluster [45–49] in the presence of the explicit PSII protein environment, using a quantum mechanical/molecular mechanical (QM/MM) approach, considering not only the Mn_4CaO_5 cluster and the ligand residues but also the second sphere residues and the H-bond network quantum chemically.

2. Computational procedures

2.1. Coordinates and atomic partial charges

The atomic coordinates of PSII were obtained from the X-ray structure of the PSII monomer unit "A" of the PSII complexes from *Thermosynechococcus vulcanus* at a resolution of 1.9 Å (PDB ID: 3ARC) [4]. Hydrogen atoms were generated and energetically optimized with CHARMM [50], while the positions of all non-hydrogen atoms were fixed, and all titratable groups were kept in their standard protonation states (i.e., acidic groups were ionized and basic groups were protonated). D1-His337 was considered to be protonated [25]. For the QM/MM calculations, we added additional counter ions to neutralize the entire system. Atomic partial charges of the amino acids were adopted from the all-atom CHARMM22 [51] parameter set. The atomic charges of the cofactors were taken from our previous studies on PSII [52].

2.2. QM/MM calculations

We employed the electrostatic embedding QM/MM scheme, in which electrostatic and steric effects created by a protein environment were explicitly considered, and we used the Qsite [53] program code, as in previous studies [54]. We employed the unrestricted DFT method with the B3LYP functional and LACVP* basis sets. To analyze the Mn_4CaO_5 geometries in S_1 and deprotonated S_0 states, the QM region was defined as the Mn_4CaO_5 cluster (including the ligand side-chains of D1-Asp170, D1-Glu189, D1-His332, D1-Glu333, D1-Asp342, and CP43-Glu354, and the backbone of D1-Ala344), the ligand water molecules of W1–W4, the O4–water chain (W538 and W539), the D1-His337 network (W370 and W387), and the O1 netwotk (W398, W778, and W923). To analyze the Mn_4CaO_5 geometries in S_{-1}, S_{-2}, and S_{-3}, and the H-bond potential-energy profiles, the QM region was defined as the Mn_4CaO_5 cluster (including the ligand side-chains of D1-Asp170, D1-Glu189, D1-His332, D1-Glu333, D1-Asp342, and CP43-Glu354, and the backbone of D1-Ala344), the ligand water molecules of W1–W4, the O4–water chain (W538 and W539), the D1-His337 network (W370 and W387), the O1 netwotk (W398, W778, and W923), the Cl-1 binding site (Cl-1, W442, W446, and the side-chains of D1-Asn181 and D2-Lys317), the second-sphere ligands (side-chains of D1-Asp61 and CP43-Arg357), the H-bond network of TyrZ (side-chains of D1-Tyr161, D1-His190, and D1-Asn298), and the diamond-shaped cluster of water molecules [52] (W5, W6, and W7). Specifically, the coordinates of the heavy atoms in the surrounding MM region were fixed at their original X-ray coordinates, while those of the H atoms in the MM region were optimized using the OPLS2005 force field. All of the atomic coordinates in the QM region were fully relaxed (i.e., not fixed) in the QM/MM calculation. All of the H-bond partners were included in the QM region, which did not hinder proton transfer along the H-bonds in calculations. The cluster was considered to comprise ferromagnetically coupled Mn atoms, where the total spin S = 14/2, 15/2, 16/2, 17/2, and 18/2 in S_1, S_0, S_{-1}, S_{-2}, and S_{-3}, respectively. We assigned the valence of Mn atoms from calculated Mulliken spin populations. Note that the resulting optimized Mn_4CaO_5 geometry appears not to be crucial to the spin configurations within the same Mn redox distribution, as demonstrated in previous theoretical studies [12,27].

2.3. H-bond potential energy

To follow the proton transfer (PT) pathways, we employed an iterative (constrained) QM/MM geometry optimization, with fixing of the selected reaction coordinate. First, we prepared the QM/MM optimized geometry without constraints, and we used the resulting geometry as the initial geometry. Next, the reaction coordinate was defined as a linear combination of two PT distances (O/N_{donor}–H and H–$O_{acceptor}$). The H atom was then moved from the H-bond donor atom (O/N_{donor}) toward the acceptor atom ($O_{acceptor}$) by 0.05 Å, and the geometry was optimized by constraining the O/N_{donor}–H and H–$O_{acceptor}$ distances in order to follow the proton motion. Next, we calculated the energy of the resulting geometry at each PT coordinate. This procedure was repeated until the H atom reached the $O_{acceptor}$ atom. Except for the atoms directly involved in the PT reaction coordinate (i.e., O/N_{donor}, transferring H, and $O_{acceptor}$ atoms), all the atomic coordinates in the QM region were fully relaxed (i.e., not fixed) in the generation of the scans.

2.4. Protonation states and H-bond partners of the Mn_4CaO_5 cluster

Previous electron spin echo envelope modulation (ESEEM) and electron nuclear double resonance (ENDOR) studies have suggested that all of the μ-oxo bridges of the Mn_4CaO_5 cluster are deprotonated in

the S_2 state [49]. Because proton release is not observed in the S_1 to S_2 transition, the ESEEM and ENDOR data thus imply that the μ-oxo bridges of the Mn_4CaO_5 cluster are already deprotonated in S_1 [45–49]. If the PSII crystal was originally in S_1 before X-ray exposure, the deprotonated Mn_4CaO_5 cluster (i.e., O1 to O5 are O^{2-}) should have been reduced during crystallographic data collection. Thus, we assumed that the μ-oxo bridges of the Mn_4CaO_5 cluster were initially fully deprotonated in S_1 and further reduced by accepting protons via the H-bonds during X-ray exposure. The possible protonation of the Mn_4CaO_5 cluster was considered to originate from the proton of the immediate proton donors.

To analyze the potential-energy profiles of the H-bonds in the Mn_4CaO_5 cluster, we considered the following bonds: O1…W923, O2…CP43-Arg357, O3…D1-His337, O4…W539, and O5…W3. Siegbahn rationalized that O5 ($=OH^-$) deprotonation occurred in the S_0 to S_1 transition, by assuming an additional water molecule near O5 in DFT calculations, which was invisible in the original PSII crystal structure [36]. If there were a properly oriented proton acceptor for O5, then it would help decrease the energy barrier for the release of a proton from O5. However, as pointed out in ref. [33], in the actual geometry of the PSII crystal structure, the water molecule cannot be placed at the corresponding position because of the presence of the hydrophobic D1-Val185 side-chain. Thus, we neither specifically modeled the corresponding water molecule nor specifically added protons in the reduced Mn_4CaO_5 cluster (e.g., at O5 in S_0).

Mn3–Mn4 is a key distance that can allow us to evaluate the reduction state of PSII crystal structures with respect to geometries obtained from ENDOR, EPR, or simulation of the EXAFS [7,9,45–47,58] in S_1. From ENDOR, EPR and simulation of the EXAFS, it has been proposed that a Mn–—Mn distance is ~2.7 Å in S_1 (2.73 Å [58], 2.72 Å [45], or 2.75 Å [46]). In the present calculations, Mn3–Mn4 was 2.76 Å in S_1.

3. Results

3.1. Overall shape of the over-reduced Mn_4CaO_5 cluster

For the deprotonated Mn_4CaO_5 cluster, the resulting Mn oxidation states (Mn1, Mn2, Mn3, Mn4) were (III, III, IV, III) in S_0, (III, III, IV, II) in S_{-1}, (III, III, III, II) in S_{-2}, and (II, III, III, II) in S_{-3} in the PSII protein environment. The overall shape of the deprotonated Mn_4CaO_5 cluster and the H-bond geometry essentially remained unchanged in S_1 [33], S_0, and S_{-1} (Fig. 3). In contrast, there were remarkable changes in the geometry when reduced from S_{-1} to S_{-2} (Fig. 3). In S_{-2}, the potential energy profile suggests that protonation of O2 by CP43-Arg357 and protonation of O3 by D1-His337 [14] can occur (Fig. 4). The most striking feature was the formation of the H-bond between O5 and W3 by donation of a H-bond from H_2O at W3 to O^{2-} at O5 (Fig. 3). As the cluster was reduced, the O5…H–O_{W3} angle of 67° in S_1 (i.e., no H-bond) was increased to 87° in S_0 (no H-bond), 109° in S_{-1} (no H-bond), and finally 151° in S_{-2}.

Protonation was not observed upon reduction of deprotonated S_1 to S_{-1} via S_0, i.e., over-reduction of deprotonated S_1 to S_0 was an electron transfer (ET) process. In contrast, the physiological S_0 to S_1 transition is a proton-coupled electron transfer (PCET) process. Thus, the Mn oxidation state in over-reduced S_0 (III, III, IV, III) was different from that in physiological S_0, (III, IV, III, III) for the O4-protonated (O4-H, e.g., [33]) and O5-protonated (O5-H, e.g., [28]) Mn_4CaO_5 clusters. The difference in the Mn oxidation state is due to the difference in the S_0 protonation state (protonated in physiological S_0 and deprotonated in over-reduced S0). Mn3(IV) was more significantly destabilized by O4-H or O5-H in physiological S_0 than by deprotonated O4 or deprotonated O5 in over-reduced S_0. The difference in the protonation state and the Mn oxidation state in S_0 also implies the irreversibility between over-reduction and physiological oxidation processes.

In S_{-2}, reduction of Mn3 makes O5 attract both Mn1(III) and the W3

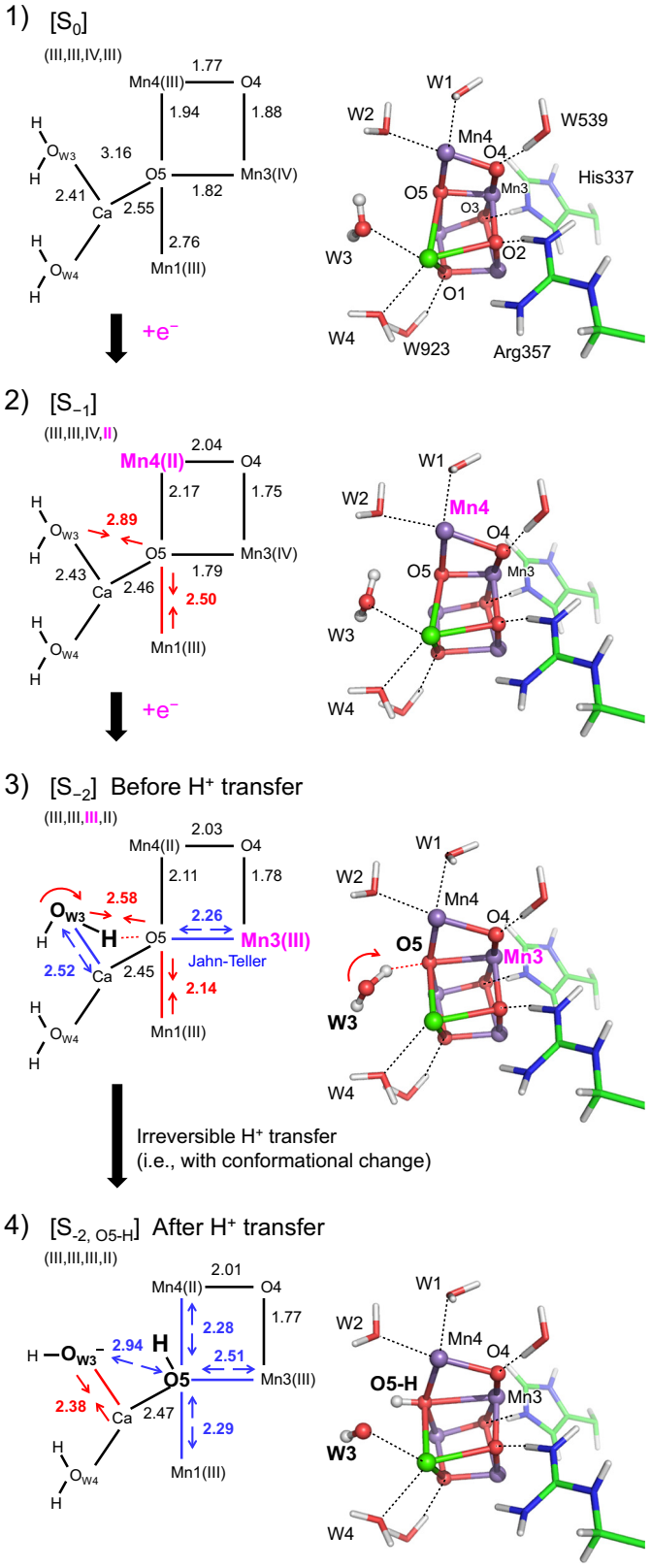

Fig. 3. Changes in the Mn_4CaO_5 geometries upon reduction (S_0, S_{-1}, and S_{-2}) and protonation ($S_{-2,O5\text{-}H}$). 1) Reduction of deprotonated S_1 (III, IV, IV, III) resulted in deprotonated S_0 (III, III, IV, III). 2) Upon reduction of S_0 to S_{-1}, Mn4(III) was preferentially reduced to Mn4(II), because Mn4 is involved in only two Mn–—O bonds. 3) In S_{-2}, W3 reorients toward O5 and donates an H-bond with O5. 4) Once proton transfer occurs and forms protonated O5, OH^- at O5 does not orient toward W3 and cannot form an H-bond with W3. See Supporting Information for the atomic coordinates.

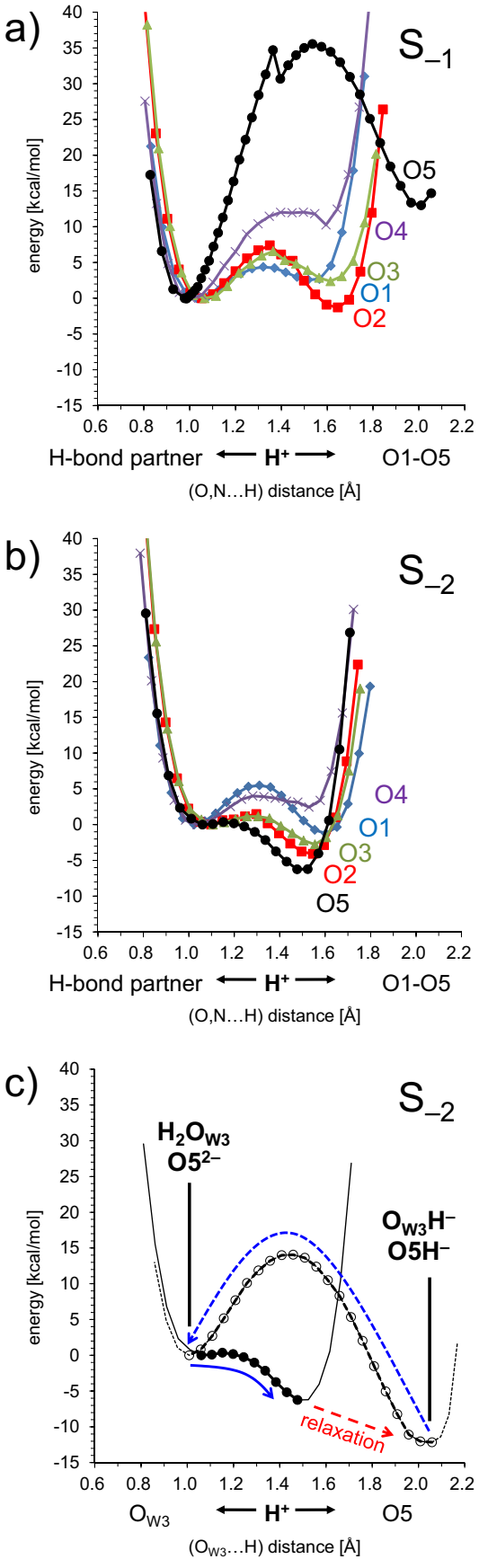

Fig. 4. The energy profiles along the proton transfer coordinate for H-bonds with deprotonated Mn_4CaO_5 cluster in a) S_{-1}. H-bonds are O1…W923 (O1), O2…CP43-Arg357 (O2), O3…D1-His337 (O3), O4…W539 (O4), and O5…W3 (O5). The energy drop in O5 is due to an alteration of an H-bond pattern in the diamond-shaped cluster of water molecules near TyrZ. b) S_{-2}. For comparison, the energy minimum in the H-bond partner moiety was set to zero. c) Heterogeneity in the energy profiles for forward proton transfer from H_2O_{W3} at Ca^{2+} to $O5^{2-}$ (solid thick curve with closed circles) and backward proton transfer from O5-H^- to $O_{W3}H^-$ (dotted thick curve with open circles) in S_{-2}. The solid and dotted arrows indicate forward and backward proton transfer, respectively. The red dotted arrow indicates the relaxation process (i.e., reorientation of OH^- at O5) after formation of OH^- at both W3 and O5.

proton more strongly (Fig. 3, panel 3), which shortens the W3–O5 bond to 2.58 Å (i.e., the W3–H…O5 H-bond forms). The short O5…O_{W3} H-bond in S_{-2} implies that the H atom is significantly migrated toward the acceptor O5 moiety. Because the characteristics of H-bonds cannot be analyzed solely by the H-bond distances, we analyzed the potential-energy profiles of the H-bonds in the Mn_4CaO_5 cluster, i.e., O1…W923, O2…CP43-Arg357, O3…D1-His337, O4…W539, and O5…W3. The potential-energy profile suggests that the energy barrier for proton transfer along the O5…O_{W3} bond is high and the Mn_4CaO_5 cluster remains deprotonated in S_{-1} (Fig. 4a). In contrast, S_{-2} strongly requires protonation at any of the five O atoms of the Mn_4CaO_5 (Fig. 4), including O5. Remarkably, the O5…O_{W3} H-bond exists in S_{-2} only before proton transfer occurs from W3 to O5 and disappears immediately afterward (Fig. 3). After protonation of O5, the H-bond disappears as indicated by an increase in the O5…O_{W3} distance from 2.58 (Fig. 3, panel 3) to 2.94 Å (Fig. 3, panel 4) and a decrease in the O5…H–O_{W3} angle from 151 to 126°. It should also be noted that all the other H-bonds remained during over-reduction.

In S_{-3}, where (Mn1, Mn2, Mn3, Mn4) = (II, III, III, II) and O5 = OH^-, protonation of O2 by the H-bond donor CP43-Arg357 and/or protonation of O3 by the H-bond donor D1-His337 occurred, resulting in three different protonation patterns, (O2–—H, O3–—H, O5–—H), (O2–—H, O5–—H), and (O3–—H, O5–—H). See Supporting Information for the atomic coordinates of the resulting QM region. These protonation states can energetically co-exist and it seems likely that the protonation pattern of the Mn_4CaO_5 cluster is not unique in S_{-3}, which might be associated with S_{-3} being the dominant over-reduced state [11].

3.2. *Mn–—O lengths in the over-reduced Mn_4CaO_5 cluster*

According to XAS studies, the PSII crystal structure may have been over-reduced during crystallographic data collection, resulting in the elongation of Mn–—O bonds [1,7–9]. Yano et al. estimated that ~25% of the Mn ions are reduced to Mn(II) in the 1.9-Å structure [8]. Mn(II), which is absent in the S state over S_0, is generated on the dangling Mn4 site upon reduction to S_{-1} and S_{-2} (Fig. 3). As proposed by XAS studies, Mn4(III)–O5 (1.94 Å in S_0) is lengthened to 2.17 Å in S_{-1} in response to the formation of Mn4(II)–O5. The same tendency also holds true for Mn4–O4, i.e., Mn4(III)–O4 = 1.94 Å in S_0 and Mn4(II)–O4 = 2.04 Å in S_{-1}.

However, it should also be noted that a long or even longest Mn–—O bond does not necessarily contain Mn(II) in the over-reduced Mn_4CaO_5 cluster. Indeed, Mn4(II)–O5 (2.17 Å) is shorter than Mn1(III)–O5 (2.50 Å) in S_{-1} (Fig. 3). Furthermore, Mn4(II)–O5 (2.17 Å in S_{-1} and 2.11 Å in S_{-2}; Fig. 3) is even shorter than Mn4–O5 (2.50 Å [4]) of the 1.9-Å structure. These facts suggest that the presence of Mn(II) should not be evaluated based only on the Mn–—O distances.

4. Discussion

The protonation of O5 by W3 upon over-reduction, as reported here, is unique since O5 has no direct H-bond partner in the original

geometry of the 1.9-Å structure [32]. To form a H-bond between O5 and W3, deformation of the Mn_4CaO_5 geometry is needed. In the deprotonated Mn_4CaO_5 cluster, reduction of S_{-1} (III, III, **IV**, II) to S_{-2} (III, III, **III**, II) occurs with reduction of Mn3(IV) to Mn3(III), which significantly lengthens the Mn3(III)–O5 bond to 2.26 Å as the Jahn-Teller axis (Fig. 3). Notably, the Mn3(III)–O5 bond length of 2.26 Å is similar to the Mn3–O5 bond lengths of 2.20 Å determined by Suga et al. [31] and 2.38 Å determined by Umena et al. [4] based on the crystal structures. Based on these results, it seems likely that the long Mn–—O5 distances in the PSII crystal structures do not necessarily be interpreted as the Mn(II)-containing over-reduced cluster or the O5-H cluster.

4.1. Mechanism of O5 protonation by W3 at Ca^{2+}

The forward proton transfer from H_2O at W3 to deprotonated O5 can occur in S_{-2}, but the backward proton transfer from OH^- at O5 to OH^- at O_{W3} is energetically disfavored because the O5…O_{W3} H-bond disappears immediately once the forward proton transfer occurs (Fig. 3). The loss of the H-bond makes proton transfer specifically to O5 in S_{-2} irreversible (even in the same S state), in contrast to proton transfer to other O sites (Fig. 4b, c). Thus, once generated, OH^- at O5 remains stable.

If a water molecule were able to access the O5 moiety, OH^- at O5 might release a proton via the water molecule. However, this is not the case for O5, because the O5 moiety is hydrophobic due to the conserved D1-Val185 side-chain being ~3.5 Å away [4,31]. In addition, there is no space near O5 to place a water molecule, as demonstrated by Siegbahn [36], who placed a water molecule at O5 only after removing the D1-Val185 side-chain and twisting the D1-His332 side-chain by 90° (discussed in refs. [33, 60]). Dynamics of D1-Val185 cannot increase the cavity space at O5. Indeed, molecular dynamics simulations using the water-removed PSII structure demonstrated that no water molecule could enter the O5 moiety even at the time scale when most of the water molecules found in the crystal structure (including those in the water channels near the Mn_4CaO_5 cluster) were reproduced [40].

The irreversible proton transfer from W3 to O5 is due to the loss of the H-bond after the forward proton transfer, which ultimately originates from the weak ligation of W3 to Ca^{2+}. Both W2 and W3 are at a distance of 3.0–3.1 Å from O5 [4]. Upon reduction to S_{-2}, W3 moved away from Ca^{2+}, reoriented toward O5, and the proton migrated significantly toward O5, being ready for proton transfer (Fig. 3), whereas W2 remained fixed. The weak binding of W3 at Ca^{2+} (with respect to W2 at Mn2) makes reorganization of W3 (i.e., reorientation of W3 and donation of a H-bond to O5) and exergonic proton transfer possible upon over-reduction.

The large mobility of a water molecule at Ca^{2+} reported here may resemble the Ca^{2+}-mediated water oxidation models in the S_2 to S_3 transition, in which a water molecule near Ca^{2+} (e.g., W3) releases a proton and is incorporated into the O5 moiety [61,62], rather than the Mn4-mediated models, in which a water molecule at Mn4 releases a proton and is incorporated into the O5 moiety [63–65]. It seems likely that in S_{-2}, interaction between the Mn4-d and W2-p orbitals makes W2 immobile with respect to W3 (Fig. 5).

In general, deprotonation of a water molecule occurs effectively when it directly binds at the redox-active site, e.g., release of the proton from protonated O4 upon oxidation of Mn3 in the S_0 to S_1 transition [33] and from W1 upon oxidation of Mn4 in the S_2 to S_3 transition [39]. In both cases, the O atom, as a deprotonation site, directly binds at Mn and form a short low-barrier H-bond with the proton acceptor (a water molecule W539 for O4 [33] and D1-Asp61 for W1 [39]). It is unclear how W3 at Ca^{2+} could deprotonate specifically in the S_2 to S_3 transition, because Ca^{2+} is never oxidized during the S-cycle. Nakamura and Noguchi proposed that oxidation of Mn1 and Mn4 would alter the polarization of the ligand residues D1-Glu189 and D1-Asp170 and decrease pK_a of W4 and W3, respectively [67], which might be a possible mechanism if W3 or W4 released the proton in the S_2 to S_3 transition.

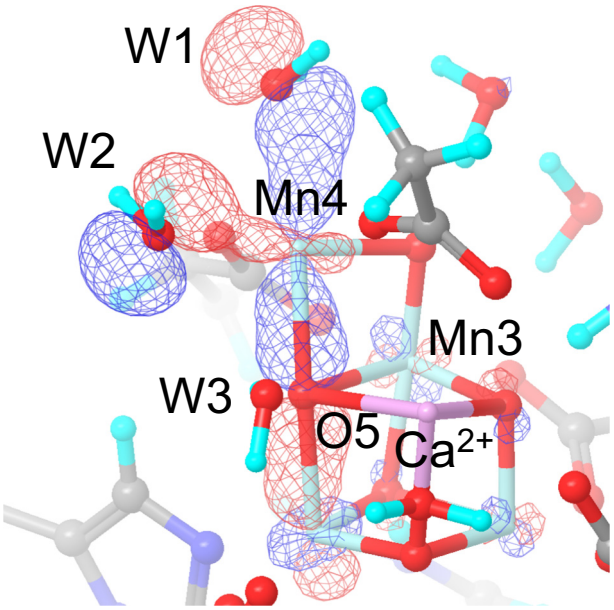

Fig. 5. The absence of molecular orbitals at the Ca^{2+} moiety in S_{-2}.

However, the decrease in pK_a of W3 at redox-inactive Ca^{2+} via changes in the polarization of D1-Asp170 is somewhat indirect and thus smaller than the decrease pK_a of W1 and W2 at redox-active Mn4. In addition, W1 at Mn4 has D1-Asp61 as a H-bond acceptor, whereas W3 has no corresponding acidic residue. These suggest that deprotonation of W3 would be a process with a high activation barrier. A proton transfer pathway via TyrZ proposed by Nakamura et al. might possibly contribute to the deprotonation of W3 [68], the mechanism of which requires the release of a proton from the closed H-bond between TyrZ and D1-His190, i.e., not the typical Grotthuss-like proton conduit.

4.2. Long O5–—Mn distances

The presence of OH^- at O5 was originally proposed for the S_1 state by Umena et al. based on the long O5–—Mn distances in the crystal structure [4]. Suga et al. also favor a model where O5 is OH^- in S_1 [31,69]. These proposed models may be in line with theoretical calculations. QM/MM studies by Shoji et al. [70] have reproduced two of the three significantly lengthened distances between O5 and the adjacent Mn ions (i.e., O5–Mn1 and O5–Mn4) in the crystal structures when assuming OH^- at O5. On the other hand, the O5–Mn3 distance (2.20 Å determined by Suga et al. [31] and 2.38 Å determined by Umena et al. [4]) were not reproduced even when O5 was assumed to be OH^- (e.g., 1.96 Å by Shoji et al. [70]), as pointed out in ref. [33]. The present QM/MM calculations resulted in the O5–Mn3 distance of 2.26 Å, which essentially reproduces the distance of ~2.3 Å determined in the crystal structures, without assuming the presence of OH^- at O5 (Fig. 3, panel 3). This suggests that a significantly lengthened O5–—Mn distance may be due to Mn(III), such that O5–Mn(III) serves as the Jahn-Teller axis.

5. Conclusions

Using QM/MM calculations, we analyzed the reduction processes of the deprotonated Mn_4CaO_5 cluster in the PSII protein environment. Upon over-reduction, W3 at Ca^{2+} reoriented toward O5, formed a H-bond with O5, and transferred a proton because of the weak binding of W3 at Ca^{2+}, whereas W2 remained immobile. The H-bond between W3 and O5 disappeared immediately after proton transfer. Thus, once generated, OH^- at O5 remained stable. The driving force for the formation of the H-bond between W3 and O5 was provided by the

reduction of Mn3(IV) to Mn3(III), the site where O5 directly binds. As viewed, O5 is easily protonated upon over-reduction, but —this does not necessarily mean that O5 is the deprotonation site in the S_0 to S_1 transition. Notably, all computational studies that suggested that O5 was the deprotonation site in the S_0 to S_1 transition were conducted using the simplified DFT models in the absence of the PSII protein environment [17,24,32,36], which cannot consider electrostatic interactions and/or hydrophobic space of key components, e.g., D1-Val185 [18], D1-Asn298 [19,20], D2-Lys317 [21], and Cl^- [22] (see Refs. [33,60]). It seems most likely that in the presence of the PSII protein environment O5 is the protonation site upon over-reduction but not the proton-releasing site in the physiological S_0 to S_1 transition.

Transparency document

The Transparency document associated with this article can be found, in online version.

Declaration of competing interest

There are no conflicts to declare.

Acknowledgment

This research was supported by JST CREST (JPMJCR1656), JSPS KAKENHI (JP18H01186 to K.S., JP16H06560 to K.S and H.I., and JP26105012 and JP18H05155 to H.I.), Japan Agency for Medical Research and Development (AMED; 18ak0101084h0002), and Interdisciplinary Computational Science Program in CCS, University of Tsukuba.

Appendix A. Supplementary data

Supplementary data to this article can be found online at https://doi.org/10.1016/j.bbabio.2019.148059.

References

[1] H. Dau, I. Zaharieva, M. Haumann, Recent developments in research on water oxidation by photosystem II, Curr. Opin. Chem. Biol. 16 (2012) 3–10.
[2] N. Cox, J. Messinger, Reflections on substrate water and dioxygen formation, Biochim. Biophys. Acta 1827 (2013) 1020–1030.
[3] J.R. Shen, The structure of photosystem II and the mechanism of water oxidation in photosynthesis, Annu. Rev. Plant Biol. 66 (2015) 23–48.
[4] Y. Umena, K. Kawakami, J.-R. Shen, N. Kamiya, Crystal structure of oxygen-evolving photosystem II at a resolution of 1.9 Å, Nature 473 (2011) 55–60.
[5] K. Kawakami, Y. Umena, N. Kamiya, J.-R. Shen, Structure of the catalytic, inorganic core of oxygen-evolving photosystem II at 1.9 Å resolution, J Photochem Photobiol B, 104 (2011) 9–18.
[6] F.H. Koua, Y. Umena, K. Kawakami, J.R. Shen, Structure of Sr-substituted photosystem II at 2.1 Å resolution and its implications in the mechanism of water oxidation, Proc. Natl. Acad. Sci. U. S. A. 110 (2013) 3889–3894.
[7] J. Yano, J. Kern, K.D. Irrgang, M.J. Latimer, U. Bergmann, P. Glatzel, Y. Pushkar, J. Biesiadka, B. Loll, K. Sauer, J. Messinger, A. Zouni, V.K. Yachandra, X-ray damage to the Mn_4Ca complex in single crystals of photosystem II: a case study for metalloprotein crystallography, Proc. Natl. Acad. Sci. U. S. A. 102 (2005) 12047–12052.
[8] J. Yano, V. Yachandra, Mn_4Ca cluster in photosynthesis: where and how water is oxidized to dioxygen, Chem. Rev. 114 (2014) 4175–4205.
[9] M. Grabolle, M. Haumann, C. Muller, P. Liebisch, H. Dau, Rapid loss of structural motifs in the manganese complex of oxygenic photosynthesis by X-ray irradiation at 10-300 K, J. Biol. Chem. 281 (2006) 4580–4588.
[10] S. Luber, I. Rivalta, Y. Umena, K. Kawakami, J.-R. Shen, N. Kamiya, G.W. Brudvig, V.S. Batista, S_1-state model of the O_2-evolving complex of photosystem II, Biochemistry 50 (2011) 6308–6311.
[11] A. Grundmeier, H. Dau, Structural models of the manganese complex of photosystem II and mechanistic implications, Biochim. Biophys. Acta 133 (2012) 88–105.
[12] W. Ames, D.A. Pantazis, V. Krewald, N. Cox, J. Messinger, W. Lubitz, F. Neese, Theoretical evaluation of structural models of the S_2 state in the oxygen evolving complex of photosystem II: protonation states and magnetic interactions, J. Am. Chem. Soc. 133 (2011) 19743–19757.
[13] Y. Kurashige, G.K. Chan, T. Yanai, Entangled quantum electronic wavefunctions of the Mn_4CaO_5 cluster in photosystem II, Nat. Chem. 5 (2013) 660–666.
[14] A. Galstyan, A. Robertazzi, E.W. Knapp, Oxygen-evolving Mn cluster in photosystem II: the protonation pattern and oxidation state in the high-resolution crystal structure, J. Am. Chem. Soc. 134 (2012) 7442–7449.
[15] M. Askerka, D.J. Vinyard, J. Wang, G.W. Brudvig, V.S. Batista, Analysis of the radiation-damage-free X-ray structure of photosystem II in light of EXAFS and QM/MM data, Biochemistry 54 (2015) 1713–1716.
[16] K. Nilsson, H.P. Hersleth, T.H. Rod, K.K. Andersson, U. Ryde, The protonation status of compound II in myoglobin, studied by a combination of experimental data and quantum chemical calculations: quantum refinement, Biophys. J. 87 (2004) 3437–3447.
[17] V. Krewald, M. Retegan, N. Cox, J. Messinger, W. Lubitz, S. DeBeer, F. Neesea, D.A. Pantazis, Metal oxidation states in biological water splitting, Chem. Sci. 6 (2015) 1676–1695.
[18] H. Bao, R.L. Burnap, Structural rearrangements preceding dioxygen formation by the water oxidation complex of photosystem II, Proc. Natl. Acad. Sci. U. S. A. 112 (2015) E6139–E6147.
[19] H. Kuroda, N. Kodama, X.-Y. Sun, S. Ozawa, Y. Takahashi, Requirement for Asn298 on D1 protein for oxygen evolution: analyses by exhaustive amino acid substitution in the green alga *Chlamydomonas reinhardtii*, Plant Cell Physiol. 55 (2014) 1266–1275.
[20] R. Nagao, H. Ueoka-Nakanishi, T. Noguchi, D1-Asn-298 in photosystem II is involved in a hydrogen-bond network near the redox-active tyrosine Y_Z for proton exit during water oxidation, J. Biol. Chem. 292 (2017) 20046–20057.
[21] H. Suzuki, J. Yu, T. Kobayashi, H. Nakanishi, P.J. Nixon, T. Noguchi, Functional roles of D2-Lys317 and the interacting chloride ion in the water oxidation reaction of photosystem II as revealed by Fourier transform infrared analysis, Biochemistry 52 (2013) 4748–4757.
[22] H. Wincencjusz, H.J. van Gorkom, C.F. Yocum, The photosynthetic oxygen evolving complex requires chloride for its redox state $S_2 \rightarrow S_3$ and $S_3 \rightarrow S_0$ transitions but not for $S_0 \rightarrow S_1$ or $S_1 \rightarrow S_2$ transitions, Biochemistry 36 (1997) 3663–3670.
[23] D.A. Pantazis, W. Ames, N. Cox, W. Lubitz, F. Neese, Two interconvertible structures that explain the spectroscopic properties of the oxygen-evolving complex of photosystem II in the S_2 state, Angew. Chem. Int. Ed. 51 (2012) 9935–9940.
[24] T. Lohmiller, V. Krewald, A. Sedoud, A.W. Rutherford, F. Neese, W. Lubitz, D.A. Pantazis, N. Cox, The first state in the catalytic cycle of the water-oxidizing enzyme: identification of a water-derived μ-hydroxo bridge, J. Am. Chem. Soc. 139 (2017) 14412–14424.
[25] S. Nakamura, T. Noguchi, Infrared determination of the protonation state of a key histidine residue in the photosynthetic water oxidizing center, J. Am. Chem. Soc. 139 (2017) 9364–9375.
[26] M. Amin, L. Vogt, W. Szejgis, S. Vassiliev, G.W. Brudvig, D. Bruce, M.R. Gunner, Proton-coupled electron transfer during the S-state transitions of the oxygen-evolving complex of photosystem II, J. Phys. Chem. B 119 (2015) 7366–7377.
[27] H. Isobe, M. Shoji, S. Yamanaka, Y. Umena, K. Kawakami, N. Kamiya, J.R. Shen, K. Yamaguchi, Theoretical illumination of water-inserted structures of the $CaMn_4O_5$ cluster in the S_2 and S_3 states of oxygen-evolving complex of photosystem II: full geometry optimizations by B3LYP hybrid density functional, Dalton Trans. 41 (2012) 13727–13740.
[28] K. Saito, H. Ishikita, Influence of the Ca^{2+} ion on the Mn_4Ca conformation and the H-bond network arrangement in photosystem II, Biochim. Biophys. Acta 1837 (2014) 159–166.
[29] J. Yang, M. Hatakeyama, K. Ogata, S. Nakamura, C. Li, Theoretical study on the role of Ca^{2+} at the S_2 state in photosystem II, J. Phys. Chem. B 118 (2014) 14215–14222.
[30] M. Amin, R. Pokhrel, G.W. Brudvig, A. Badawi, S.S. Obayya, Effect of chloride depletion on the magnetic properties and the redox leveling of the oxygen-evolving complex in photosystem II, J. Phys. Chem. B 120 (2016) 4243–4248.
[31] M. Suga, F. Akita, K. Hirata, G. Ueno, H. Murakami, Y. Nakajima, T. Shimizu, K. Yamashita, M. Yamamoto, H. Ago, J.R. Shen, Native structure of photosystem II at 1.95 Å resolution viewed by femtosecond X-ray pulses, Nature 517 (2015) 99–103.
[32] R. Pal, C.F. Negre, L. Vogt, R. Pokhrel, M.Z. Ertem, G.W. Brudvig, V.S. Batista, S-state model of the oxygen-evolving complex of photosystem II, Biochemistry 52 (2013) 7703–7706.
[33] K. Saito, A.W. Rutherford, H. Ishikita, Energetics of proton release on the first oxidation step in the water-oxidizing enzyme, Nat. Commun. 6 (2015) 8488.
[34] T. Takaoka, N. Sakashita, K. Saito, H. Ishikita, pK_a of a proton-conducting water chain in photosystem II, J. Phys. Chem. Lett. 7 (2016) 1925–1932.
[35] T. Shimizu, M. Sugiura, T. Noguchi, Mechanism of proton-coupled electron transfer in the S_0-to-S_1 transition of photosynthetic water oxidation as revealed by time-resolved infrared spectroscopy, J. Phys. Chem. B 122 (2018) 9460–9470.
[36] P.E. Siegbahn, Water oxidation mechanism in photosystem II, including oxidations, proton release pathways, O-O bond formation and O_2 release, Biochim. Biophys. Acta 1827 (2013) 1003–1019.
[37] C. Zhang, C. Chen, H. Dong, J.R. Shen, H. Dau, J. Zhao, Inorganic chemistry. A synthetic Mn_4Ca-cluster mimicking the oxygen-evolving center of photosynthesis, Science 348 (2015) 690–693.
[38] C. Chen, Y. Chen, R. Yao, Y. Li, C. Zhang, Artificial Mn_4Ca clusters with exchangeable solvent molecules mimicking the oxygen-evolving center in photosynthesis, Angew. Chem. Int. Ed. 58 (2019) 3939–3942.
[39] K. Kawashima, T. Takaoka, H. Kimura, K. Saito, H. Ishikita, O_2 evolution and recovery of the water-oxidizing enzyme, Nat. Commun. 9 (2018) 1247.
[40] N. Sakashita, H.C. Watanabe, T. Ikeda, K. Saito, H. Ishikita, Origins of water molecules in the photosystem II crystal structure, Biochemistry 56 (2017) 3049–3057.
[41] H. Ishikita, W. Saenger, B. Loll, J. Biesiadka, E.-W. Knapp, Energetics of a possible proton exit pathway for water oxidation in photosystem II, Biochemistry 45 (2006) 2063–2071.

[42] C.L. Perrin, J.B. Nielson, "Strong" hydrogen bonds in chemistry and biology, Annu. Rev. Phys. Chem. 48 (1997) 511–544.
[43] C.N. Schutz, A. Warshel, The low barrier hydrogen bond (LBHB) proposal revisited: the case of the Asp... His pair in serine proteases, Proteins, 55 (2004) 711–723.
[44] H. Ishikita, K. Saito, Proton transfer reactions and hydrogen-bond networks in protein environments, J. R. Soc. Interface 11 (2014) 20130518.
[45] J.H. Robblee, J. Messinger, R.M. Cinco, K.L. McFarlane, C. Fernandez, S.A. Pizarro, K. Sauer, V.K. Yachandra, The Mn cluster in the S_0 state of the oxygen-evolving complex of photosystem II studied by EXAFS spectroscopy: are there three di-μ-oxo-bridged Mn_2 moieties in the tetranuclear Mn complex? J. Am. Chem. Soc. 124 (2002) 7459–7471.
[46] L.V. Kulik, B. Epel, W. Lubitz, J. Messinger, Electronic structure of the Mn_4O_xCa cluster in the S_0 and S_2 states of the oxygen-evolving complex of photosystem II based on pulse ^{55}Mn-ENDOR and EPR spectroscopy, J. Am. Chem. Soc. 129 (2007) 13421–13435.
[47] H. Dau, M. Haumann, The manganese complex of photosystem II in its reaction cycle? Basic framework and possible realization at the atomic level, Coord. Chem. Rev. 252 (2008) 273–295.
[48] R.D. Britt, K.A. Campbell, J.M. Peloquin, M.L. Gilchrist, C.P. Aznar, M.M. Dicus, J. Robblee, J. Messinger, Recent pulsed EPR studies of the photosystem II oxygen-evolving complex: implications as to water oxidation mechanisms, Biochim. Biophys. Acta 1655 (2004) 158–171.
[49] L. Rapatskiy, N. Cox, A. Savitsky, W.M. Ames, J. Sander, M.M. Nowaczyk, M. Rögner, A. Boussac, F. Neese, J. Messinger, W. Lubitz, Detection of the water-binding sites of the oxygen-evolving complex of photosystem II using W-band ^{17}O electron-electron double resonance-detected NMR spectroscopy, J. Am. Chem. Soc. 134 (2012) 16619–16634.
[50] B.R. Brooks, R.E. Bruccoleri, B.D. Olafson, D.J. States, S. Swaminathan, M. Karplus, CHARMM: a program for macromolecular energy minimization and dynamics calculations, J. Comput. Chem. 4 (1983) 187–217.
[51] A.D. MacKerell, Jr., D. Bashford, R.L. Bellott, R.L. Dunbrack, Jr., J.D. Evanseck, M.J. Field, S. Fischer, J. Gao, H. Guo, S. Ha, D. Joseph-McCarthy, L. Kuchnir, K. Kuczera, F.T.K. Lau, C. Mattos, S. Michnick, T. Ngo, D.T. Nguyen, B. Prodhom, W.E. Reiher, III, B. Roux, M. Schlenkrich, J.C. Smith, R. Stote, J. Straub, M. Watanabe, J. Wiorkiewicz-Kuczera, D. Yin, M. Karplus, All-atom empirical potential for molecular modeling and dynamics studies of proteins, J. Phys. Chem. B, 102 (1998) 3586–3616.
[52] K. Saito, J.-R. Shen, T. Ishida, H. Ishikita, Short hydrogen-bond between redox-active tyrosine Y_Z and D1-His190 in the photosystem II crystal structure, Biochemistry 50 (2011) 9836–9844.
[53] QSite, version 5.8, Schrödinger, LLC, New York, NY, 2012.
[54] K. Saito, T. Ishida, M. Sugiura, K. Kawakami, Y. Umena, N. Kamiya, J.-R. Shen, H. Ishikita, Distribution of the cationic state over the chlorophyll pair of photosystem II reaction center, J. Am. Chem. Soc. 133 (2011) 14379–14388.
[58] M.J. Baldwin, T.L. Stemmler, P.J. Riggs-Gelasco, M.L. Kirk, J.E. Penner-Hahn, V.L. Pecoraro, Structural and magnetic effects of successive protonations of oxo bridges in high-valent manganese dimers, J. Am. Chem. Soc. 116 (1994) 11349–11356.
[60] H. Ishikita, Protein environment that facilitates proton Transfer and electron transfer in photosystem II, in: Oxygen Production and Reduction in Artificial and Natural Systems, 2019, pp. 191–208.
[61] M. Shoji, H. Isobe, K. Yamaguchi, QM/MM study of the S_2 to S_3 transition reaction in the oxygen-evolving complex of photosystem II, Chem. Phys. Lett. 636 (2015) 172–179.
[62] I. Ugur, A.W. Rutherford, V.R.I. Kaila, Redox-coupled substrate water reorganization in the active site of photosystem II—the role of calcium in substrate water delivery, Biochim. Biophys. Acta 1857 (2016) 740–748.
[63] M. Askerka, D.J. Vinyard, G.W. Brudvig, V.S. Batista, NH_3 binding to the S_2 state of the O_2-evolving complex of photosystem II: analogue to H_2O binding during the $S_2 \rightarrow S_3$ transition, Biochemistry 54 (2015) 5783–5786.
[64] M. Retegan, V. Krewald, F. Mamedov, F. Neese, W. Lubitz, N. Cox, D.A. Pantazis, A five-coordinate Mn(IV) intermediate in biological water oxidation: spectroscopic signature and a pivot mechanism for water binding, Chem. Sci. 7 (2016) 72–84.
[65] M. Capone, D. Narzi, D. Bovi, L. Guidoni, Mechanism of water delivery to the active site of photosystem II along the S_2 to S_3 transition, J. Phys. Chem. Lett. 7 (2016) 592–596.
[67] S. Nakamura, T. Noguchi, Quantum mechanics/molecular mechanics simulation of the ligand vibrations of the water-oxidizing Mn_4CaO_5 cluster in photosystem II, Proc. Natl. Acad. Sci. U. S. A. 113 (2016) 12727–12732.
[68] S. Nakamura, R. Nagao, R. Takahashi, T. Noguchi, Fourier transform infrared detection of a polarizable proton trapped between photooxidized tyrosine Y_Z and a coupled histidine in photosystem II: relevance to the proton transfer mechanism of water oxidation, Biochemistry 53 (2014) 3131–3144.
[69] M. Suga, F. Akita, M. Sugahara, M. Kubo, Y. Nakajima, T. Nakane, K. Yamashita, Y. Umena, M. Nakabayashi, T. Yamane, T. Nakano, M. Suzuki, T. Masuda, S. Inoue, T. Kimura, T. Nomura, S. Yonekura, L.J. Yu, T. Sakamoto, T. Motomura, J.H. Chen, Y. Kato, T. Noguchi, K. Tono, Y. Joti, T. Kameshima, T. Hatsui, E. Nango, R. Tanaka, H. Naitow, Y. Matsuura, A. Yamashita, M. Yamamoto, O. Nureki, M. Yabashi, T. Ishikawa, S. Iwata, J.R. Shen, Light-induced structural changes and the site of O=O bond formation in PSII caught by XFEL, Nature, 543 (2017) 131–135.
[70] M. Shoji, H. Isobe, S. Yamanaka, M. Suga, F. Akita, J.-R. Shen, K. Yamaguchi, Theoretical studies of the damage-free S_1 structure of the $CaMn_4O_5$ cluster in oxygen-evolving complex of photosystem II, Chem. Phys. Lett. 623 (2015) 1–7.